

PAPER

An optical-transparent metamaterial for high-efficiency microwave absorption and low infrared emission

To cite this article: Cuijian Xu *et al* 2020 *J. Phys. D: Appl. Phys.* **53** 135109

View the [article online](#) for updates and enhancements.

You may also like

- [A low-profile consolidated metastructure for multispectral signature management](#)
Nitish Kumar Gupta, Gaganpreet Singh, Harshawardhan Wanare *et al.*
- [Transmission frequency variable stealth radome using the mutual inductance effect for two frequency selective surfaces](#)
Dae-Sung Son, Jong-Min Hyun and Jung-Ryul Lee
- [Stealth Coronal Mass Ejections from Active Regions](#)
Jennifer O'Kane, Lucie Green, David M. Long *et al.*



ECS
The
Electrochemical
Society
Advancing solid state &
electrochemical science & technology

DISCOVER
how sustainability
intersects with
electrochemistry & solid
state science research

An optical-transparent metamaterial for high-efficiency microwave absorption and low infrared emission

Cuilian Xu¹, Binke Wang¹, Mingbao Yan¹, Yongqiang Pang², Wenjie Wang¹, Yueyu Meng¹, Jiafu Wang¹ and Shaobo Qu¹

¹ Department of Basic Science, Air Force Engineering University, Xi'an 710051, People's Republic of China

² School of Electronics and Information Engineering, Xi'an Jiaotong University, Xi'an 710049, People's Republic of China

E-mail: wbk93@163.com and qushaobo@mail.xjtu.edu.cn

Received 31 August 2019, revised 12 December 2019

Accepted for publication 23 December 2019

Published 22 January 2020



CrossMark

Abstract

An optically transparent metamaterial structure with simultaneously broadband microwave absorptivity and low infrared (IR) emissivity is proposed. Two specifically designed optically transparent metasurfaces were combined to realize radar and IR bi-stealth. One was designed to control the microwave absorption through properly modifying the impedance and resonance peaks of the meta-atom. The other was designed to control the IR radiation. Within a wide incident angle of $\pm 60^\circ$, the proposed structure displays high absorptivity greater than 90% in the region of 6.28–12.29 GHz for TE polarization. For TM polarization, the absorptivity in the region of 7.19–15.26 GHz is greater than 90%. The IR emissivity of the metamaterial structure is about 0.30 in the IR region from 3 μm to 14 μm . The perfect consistency between experimental results and simulation results demonstrates that the proposal has practical application of multispectral stealth technology.

Keywords: metamaterial, optical transparency, radar-infrared stealth-compatibility

(Some figures may appear in colour only in the online journal)

1. Introduction

With the development of precision guidance and composite detection technologies, radar and infrared (IR) stealth compatible techniques have attracted considerable attention [1–9]. Generally, low reflectivity and high absorptivity are demanded in radar stealth, while high reflectivity and low absorptivity are required in IR stealth. It seems to be incompatible to realize radar and IR stealth using the same material. In recent years, many works have been done to resolve this problem. Liu [10] prepared $\text{La}_{1-x}\text{Ca}_x\text{MnO}_3$ ($0 \leq x \leq 0.5$) with perovskite-type structure by sol-gel method, the incorporation of Ca in LaMnO_3 leads to the decrease of electrical conductivity, while the IR emissivities are decreased. Microwave absorptivity enhanced by doping Ca^{2+} , but the width of microwave absorption band is very narrow. Based on the principles

of distributed Bragg reflector micro-cavity, Wang [11] proposed a new type of 1D Ge-ZnS photonic crystal (PC), which comprises four PCs with different thickness. The proposed PC can exhibit a near 100% reflectance in 3 μm –5 μm and 8 μm –14 μm wave band. Combining these proposed structures with radar absorbing materials, radar-IR stealth-compatibility materials can be obtained. However, the author did not further study the compatibility of the structure with radar stealth materials.

In the previous works, the high-efficiency radar absorption and low IR emissivity properties of these structures are difficult to realize simultaneously and manipulate independently. In recent years, metamaterials have attracted considerable attention in stealth technic due to their promising performances in manipulating electromagnetic (EM) waves. Various functional devices have been proposed to realize

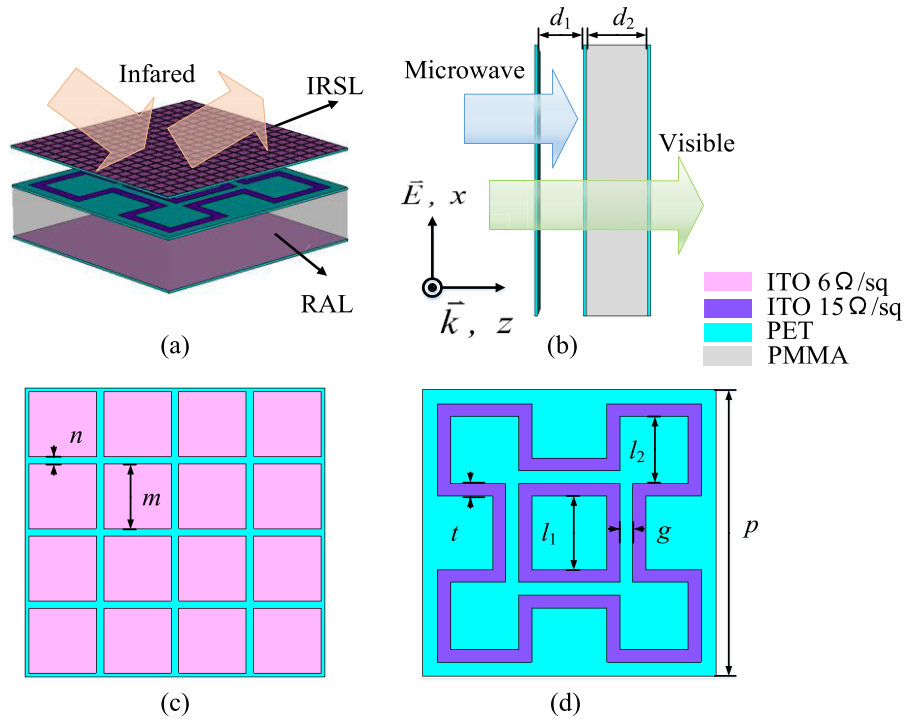


Figure 1. (a) Perspective view. (b) Side view of the radar-IR bi-stealth structure. (c) Top view of the IRSL structure. (d) Top view of the RAL structure.

perfect metamaterial absorbers, low-scattering materials and cloaks [12–19]. Compared to traditional complex materials, metamaterials which have excellent frequency selection characteristics possess more freedoms for multifunctional stealth technology. Cheng first proposed to cover a high-efficiency microwave transmission frequency selective surface (FSS) on the microwave absorbing material, the low IR emissivity could be obtained through a high-filling-ratio metallic material of the FSS [20]. Using the similar technical solution, Zhang and Cui achieved broadband absorptivity greater than 90% in the microwave region from 8.2 to 16.0 GHz and low IR emissivity from 8 μm to 14 μm. Pang and Qu designed a hybrid metasurface which can simultaneously reduce the IR emission and the microwave reflection, the principle of microwave reflection reduction is the phase cancellation, while the low IR emission arises from the high-efficiency reflection and mainly depends on the filling ration of metal in the top layer [21]. But these structures do not have optically transparent property and the microwave absorptivity at wide incident angles is low. Under special conditions, like windows on the aircrafts or cars, the stealth materials should be optically transparent. Many techniques have been proposed to realize optically transparent metamaterial absorbers and microwave scattering reduction metasurfaces [22–27]. However, little attention has been paid to their IR stealth properties.

With the help of transparent conductive indium-tin-oxide (ITO), we designed a new transparent radar-IR bi-stealth metamaterial structure. Broadband microwave absorption was achieved by overlapping three high absorption peaks. Within a wide incident angle of ±40°, the absorptivity of the proposed structure is larger than 90% in the region of 6–18 GHz. A low

emissivity of 0.30 is obtained in the IR band from 3 μm to 14 μm by adjusting the filling ratio of the ITO part. Both simulation and measurement results demonstrate the validity of the proposed optically transparent radar-IR stealth-compatibility structure, which has promising applications in multifunctional stealth fields.

2. Design and simulation

Due to the completely opposite stealth principles at microwave and IR wavelength bands, the radar-IR stealth-compatibility structure is composed of a radar absorption layer (RAL) and an infrared shielding layer (IRSL). The key factor is to design a transparent IRSL with high transmissivity at microwave band. Here, the IRSL is implemented by using capacitive FSS due to the low-pass filtering characteristic. In addition, the low IR emissivity could be obtained through a high-filling-ratio metallic material of the structure. Specifically, the emissivity ε can be calculated as [28]

$$\varepsilon = \varepsilon_m f_m + \varepsilon_d (1 - f_m) \quad (1)$$

where ε is the emissivity of the structure, the ε_m and ε_d are the emissivities of the metal and dielectric board, respectively, f_m is the filling ratio (metal area/total area) of the metal part. The emissivity of the metal is relatively low, generally lower than 0.1. The emissivity of the dielectric is high, generally greater than 0.8. Obviously, the larger the metallic material filling ratio is, the lower the IR emissivity. Thus, the low emissivity of IRSL could be realized by proper design of the FSS pattern. ITO film technology has developed rapidly with the stealth needs of optically transparent windows for weapons. ITO is

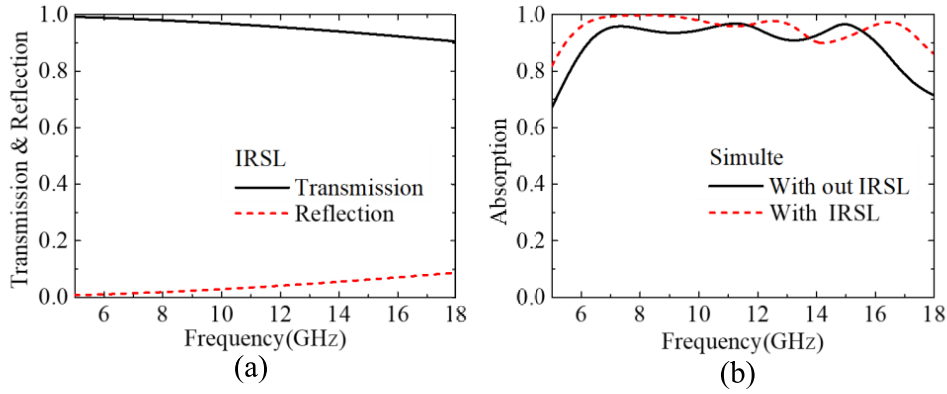


Figure 2. (a) Simulate transmission and reflection of the IRSL. (b) Simulate absorption under normal incidence.

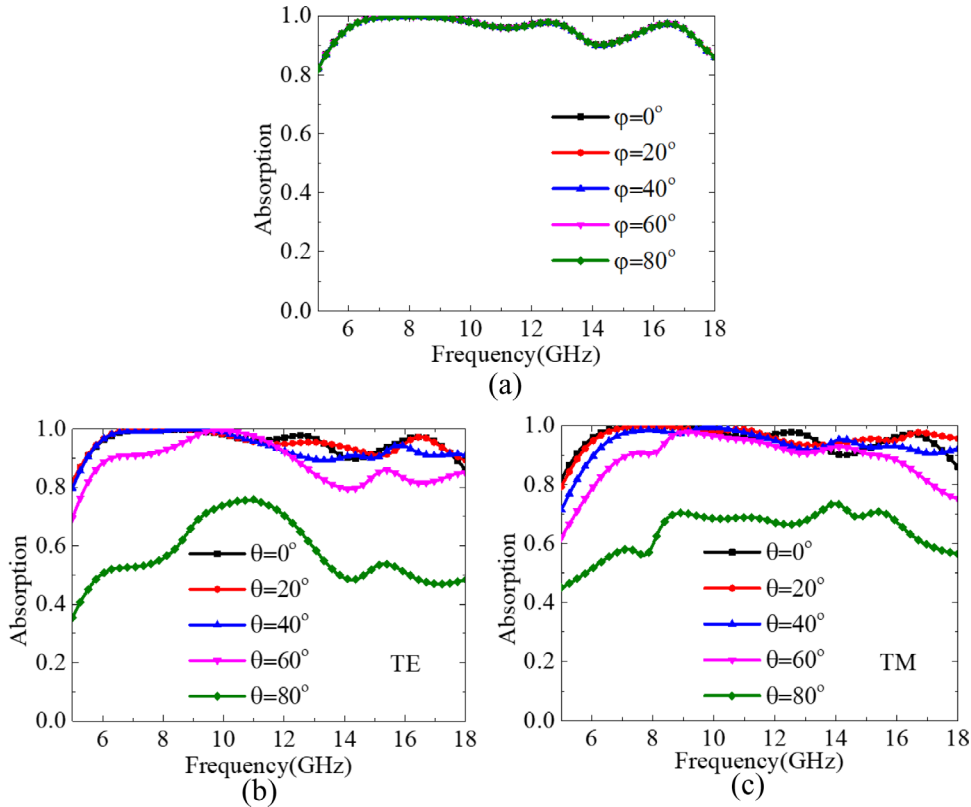


Figure 3. (a) Simulate absorption at different azimuthal angles φ for TE polarized. (b) Simulated absorption at different incident angles θ for TE polarized and (c) TM polarized.

transparent in the visible range, and the permittivity in the IR band can be expressed by Drude model [29]

$$\varepsilon(\omega) = \varepsilon_b - \frac{\omega_p^2}{\omega(\omega + i\omega_c)} \quad (2)$$

where $\varepsilon_b = 3.9$, the plasma frequency $\omega_p = 461$ THz, the collision frequency $\omega_c = 28.7$ THz. So the real part of permittivity is negative, indicating that the ITO behaves like a metal in IR band.

In order to achieve high optical light transmissivity, the constituent material components of the whole structure are selected to be optical-transparent. Different layers of the structure are stuck on transparent conductive ITO which is deposited on transparent polyethylene terephthalate (PET)

substrate with different surface resistances, as shown in figures 1(a) and (b). The periodic square ITO patch structure unit with high filling-ratio characteristics was used as FSS on the top layer to achieve high reflection of IR waves and high transmission of radar waves. It is known that the IR emissivity of ITO film decreases as the sheet resistance increases. The sheet resistance of ITO is $6.0 \Omega \text{ sq}^{-1}$ for IRSL. Figure 1(c) presents a top view of the IRSL structure, the width of the gap is $n = 0.1$ mm, and width of ITO patch is $m = 0.9$ mm, and the corresponding ITO filling ratio is 81%. The emissivity of ITO is less than 0.1, and the emissivity of the dielectric PET is less than 0.9 [29], According to equation (1), the estimated IR emissivity is approximately 0.252. Figure 1(d) presents the top view of the RAL structure. The typical RAL consists of

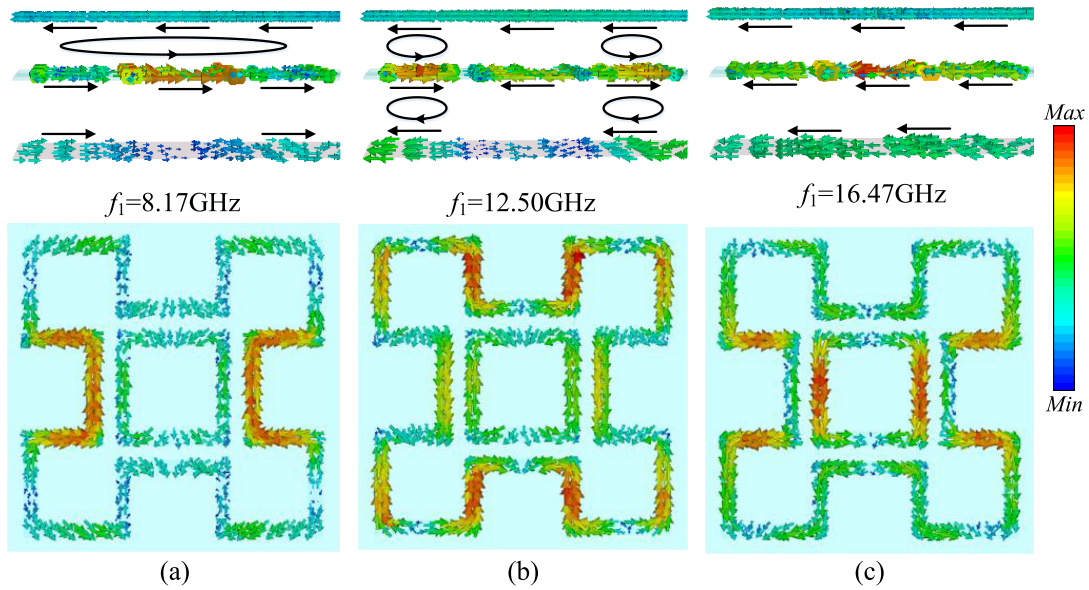


Figure 4. Top view and side view distributions of the surface currents at the resonance frequencies of: (a) 8.17 GHz, (b) 12.50 GHz, and (c) 16.47 GHz.

ITO square ring-shaped patterns placed on ITO ground film. They are separated by a polymethyl methacrylate (PMMA) spacer with a dielectric constant of 2.25 and loss tangent of 0.001. The thickness of PMMA is d_2 . The dielectric constant of PET is $3.0(1 - j0.06)$ [30]. The thickness of PET substrate is 0.175 mm. The sheet resistances of ITO patterns and ITO backing ground for RAL are $15 \Omega \text{ sq}^{-1}$ and $6.0 \Omega \text{ sq}^{-1}$, respectively. The IRSL and RAL are separated by air with each other at distance d_1 . The optimized structural parameters are $d_1 = 3.0 \text{ mm}$, $d_2 = 4.0 \text{ mm}$, $l_1 = 4.6 \text{ mm}$, $l_2 = 4.0 \text{ mm}$, $g = 0.8 \text{ mm}$, $t = 0.8 \text{ mm}$, $p = 18 \text{ mm}$. The scattering parameters were calculated using the CST Microwave Studio software. The unit cell boundary conditions are set in x - y plane, while the open boundary condition is chosen in z direction. The EM-wave absorption can be defined as $A = 1 - R - T = 1 - |S_{11}|^2 - |S_{21}|^2$, where $|S_{11}|^2$ and $|S_{21}|^2$ are the reflectivity and transmissivity, respectively. Since the surface resistance of the ITO ground film is $6.0 \Omega \text{ sq}^{-1}$, the averaged transmissivity at normal incidence is approximately zero.

Figure 2(a) shows transmission and reflection of the IRSL under normal incidence. It can be observed that the transmissivity is greater than 0.91, while reflectivity is lower than 0.08. Thus the IRSL can be regarded as a high-efficiency microwave transmission FSS within the frequencies lower than 18 GHz. Figure 2(b) shows absorption results of the structure under normal incidence. It can be observed that the designed structure can achieve high-efficiency broadband microwave absorption. Under normal incidence, the absorptivity is greater than 90% in the microwave band of 5.47–17.64 GHz. After the FSS is covered on the radar absorber, the absorption performance is significantly improved compared with the structure without the IRSL, and the absorption peak shifts to the high frequency direction. This can be clarified by the mutual coupling between the two layers. The stability of absorption with different azimuthal angles φ at $\theta = 0^\circ$ for TE polarization was investigated in figure 3(a). It can be seen that the intensity of

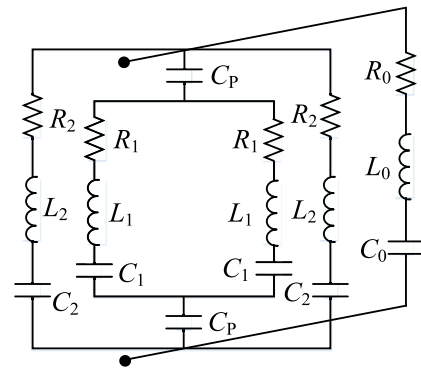


Figure 5. Equivalent RLC circuit of the proposed structure.

absorption is stable under different azimuthal angles from 0° to 85° . It reveals that the proposed structure is nearly polarization independent. The wide incident angles absorption performance is shown in figures 3(b) and (c). For both TE and TM polarizations, the absorptivity degrades gradually as the incident angle increased. However, it still has a high absorption at incident angles of 0° – 70° for both polarizations. Within a wide incident angle of $\pm 60^\circ$, the proposed structure displays high absorptivity greater than 90% in the region of 6.28–12.29 GHz for TE polarization. For TM polarization, the absorptivity in the region of 7.19–15.26 GHz is greater than 90%. Within a wide incident angle of $\pm 40^\circ$, the absorptivity in the region of 6.0–18.0 GHz is larger than 90% for both TE and TM polarization.

To reveal the absorption physical mechanism of the transparent radar-IR bi-stealth metamaterial structure, the distributions of surface currents at the resonance frequencies of 8.17, 12.50 and 16.47 GHz are shown in figure 4. Due to the IRSL is closed to the upper ITO surface of RAL, near field coupling can be induced that make it easily to excite anti-parallel currents between them. As shown in figure 4(a), at the lowest absorption band approaching 8.17 GHz, the currents are mainly

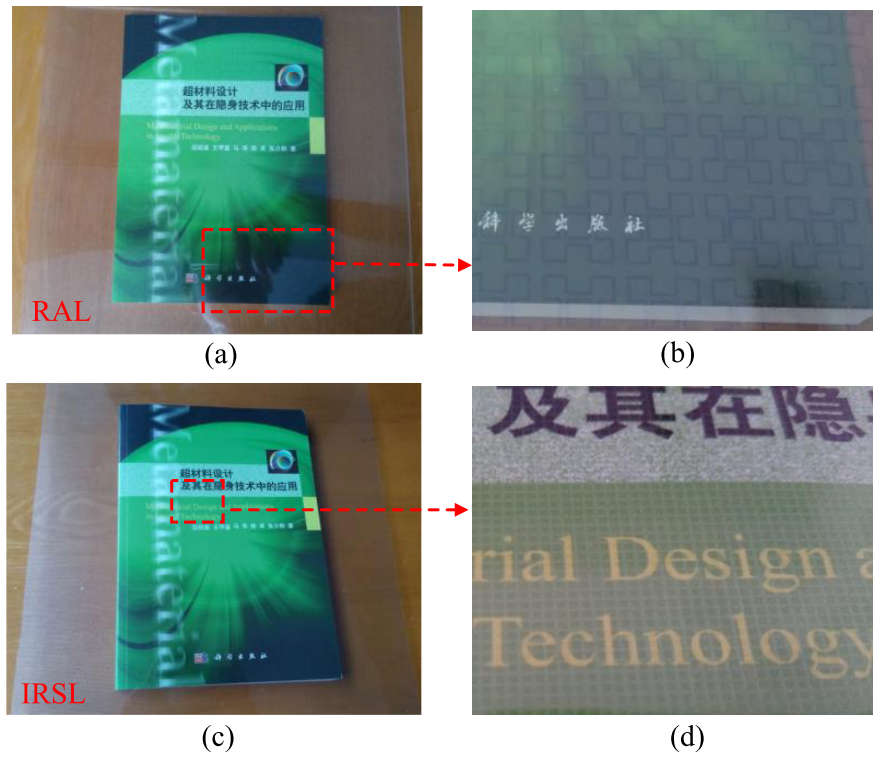


Figure 6. (a) The photograph of the fabricated RAL. (b) A larger version of RAL. (c) The photograph of the fabricated IRSL. (d) A larger version of IRSL.

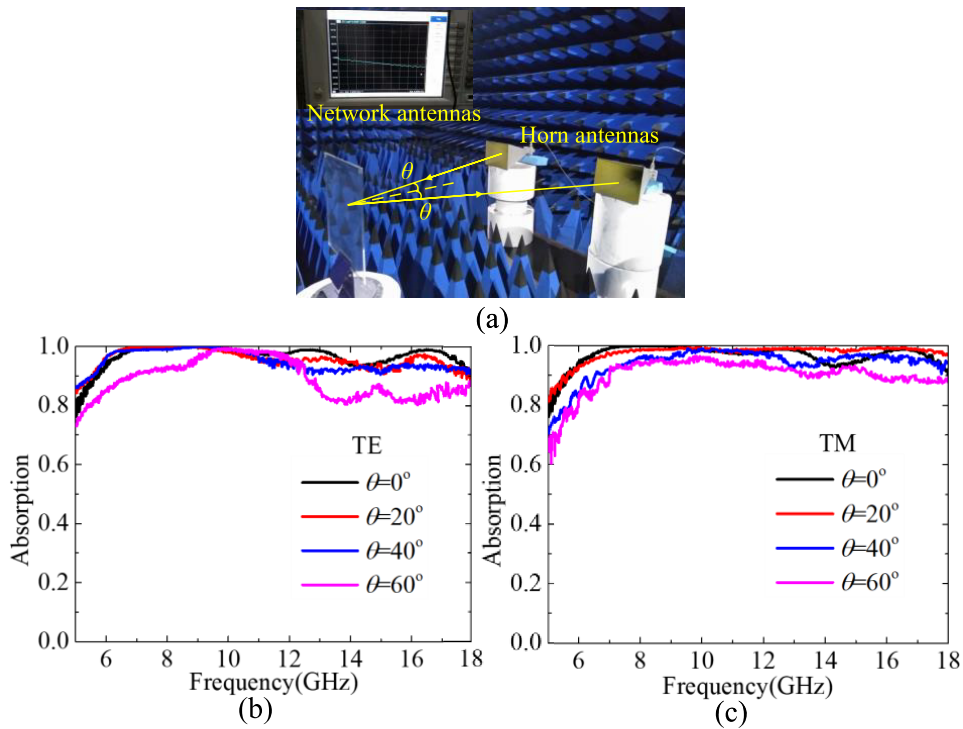


Figure 7. (a) Real pictures of the experimental setup for the microwave absorption. (b) Measured absorption at different incident angles for TE polarized and (c) TM polarized.

confined at the center position of the outer ring. Approaching 12.50 GHz and 16.47 GHz, the excited currents are enhanced at different positions of the rings. The side views of the surface currents are also displayed in figure 4. At the absorption band of 8.17 GHz, the generated surface currents on the IRSL

are anti-parallel to the upper ITO surface of RAL. Magnetic dipole is formed, and induces strong magnetic responses. In the middle absorption band approaching 12.50 GHz, anti-parallel currents were generated between the three ITO layers at the current-enhanced position. For the highest

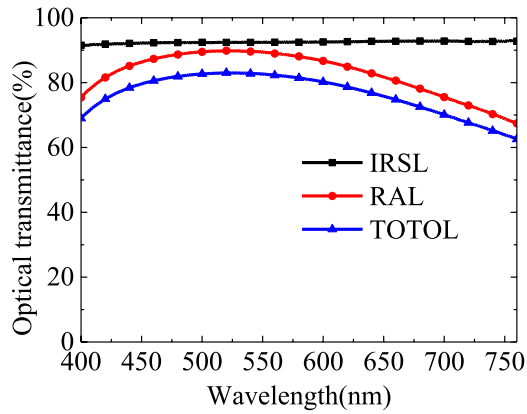


Figure 8. Measured optical transmittances of the RAL, IRSL and the TOTAL sample.

absorption band near 16.47 GHz, the excited currents are mainly focused on the upper surface of RAL. That is because the distance between the IRSL and RAL is not thin enough to its resonance wavelength. In general, the high broadband absorption mainly caused by the ohmic loss of the ITO film combining with the surface current focused on the upper layer of RAL. The surface current and the ohmic loss of the ITO film following the equation $P_{\text{loss}} = I^2R$, where I is the excited current and R is the effective surface resistance.

The equivalent RLC circuit model [31–34] of the RAL is present to analyze the absorption characteristics of the proposed structure in figure 5. In this circuit model, L_1 and C_1 are associated with the effective inductance and capacitance of the inner set of the unit cell, whereas L_2 and C_2 are viewed as the effective inductance and capacitance of the outer set. C_0 is the effective dielectric capacitance between the top metallic patch and bottom ground plate. C_p is the coupling capacitance between the outer and inner unit cell. L_0 accounts for the thin dielectric slab backed by a conducting plate. In addition, the ITO and spacer can result in ohmic and dielectric losses, respectively, so equivalent resistors of R_1 , R_2 and R_0 are introduced in each loop. The equivalent impedance of a lossy FSS can be represented through a series of RLC circuits [35]

$$Z_{\text{FSS}} = R + j\omega L + \frac{1}{j\omega C}. \quad (3)$$

For ease of calculation, the mutual inductance between the outer and inner set of unit cell has been neglected. Then the equivalent impedance of the circuit $Z(\omega)$ can be expressed [36]

$$Z(\omega) = \left[\left(\frac{R_2}{2} + j\omega \frac{L_2}{2} + \frac{1}{j\omega(2C_2)} \right) \parallel \left(\frac{R_1}{2} + j\omega \frac{L_1}{2} + \frac{1}{j\omega(2C_1)} + \frac{1}{j\omega(C_p/2)} \right) \right] \parallel \left(R_0 + j\omega L_0 + \frac{1}{j\omega C_0} \right). \quad (4)$$

According to the impedance matching theory, at the absorption frequency, the imaginary part of the equivalent surface admittance should be zero. Thus, the absorption frequency can be derived from

$$\text{Im} \left\{ \frac{1}{z(\omega)} \right\} = 0. \quad (5)$$

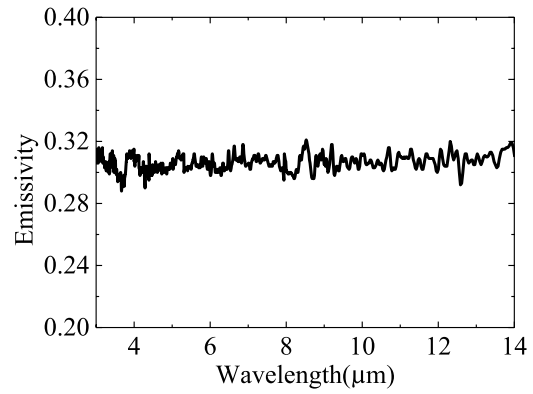


Figure 9. Measured emissivity spectra of the fabricated IRSL in the IR band.

3. Experimental results

We proceed to validate the simulate results mentioned above. A conductive ITO film deposited on optical transparent PET substrate was etched into the optimized structure by the laser etching technique. Another ITO-coated-PET sheet was used as backplane. The radar absorber was then obtained by sticking them on the sides of the PMMA board together. The IRSL is also fabricated by laser etching with high precision based on conductive ITO-coated-PET thin films. The fabricated samples with the dimension of $300 \times 300 \text{ mm}^2$ were shown in figure 6. Figure 6 shows the real photographs of books through the fabricated structure. Both the RAL and the IRSL are very clear to our naked eyes. The microwave absorption spectra are carried out by an Agilent N5224A network analyzer which is setting in microwave anechoic chamber. Three pairs of broadband antenna horns working in the frequencies of 4–8, 8–12 and 12–18 GHz acted as EM wave transmitters and receivers. Real pictures of the measurement location are shown in figure 7(a), the distance from the position of the sample plate to both horn antennas was the same. When conducting the measurements, the reflection of a metal plate with the same size as the artificial structure is first measured to normalize. The measured absorption spectra of different incident angles of TE and TM polarization were shown in figures 7(b) and (c). As expected, the measured results are consistent with the simulated results.

In this part, the optical transparency and IR emissivity of the proposed radar-IR stealth- compatibility structure are discussed. The transparent ITO film, PET substrates and loss dielectric PMMA are adopted to ensure optical transparency. To get precise characterize of the optically transparent, the optical transmittances spectra of each fabricated layer are measured using ultraviolet–visible spectrophotometer. As shown in figure 8, the average optical transmittances of the IRSL and RAL are about 92.52% and 81.10%. The total transmittance of the radar-IR stealth- compatibility structure is about 75.02%. We can improve the optical transmittance of the IRSL via reducing the ITO filling ratio. However, the reduction of the ITO filling ratio will result in the decrease of the emissivity.

Due to the large difference between the operating wavelength of EM waves and the size of structural units, it is

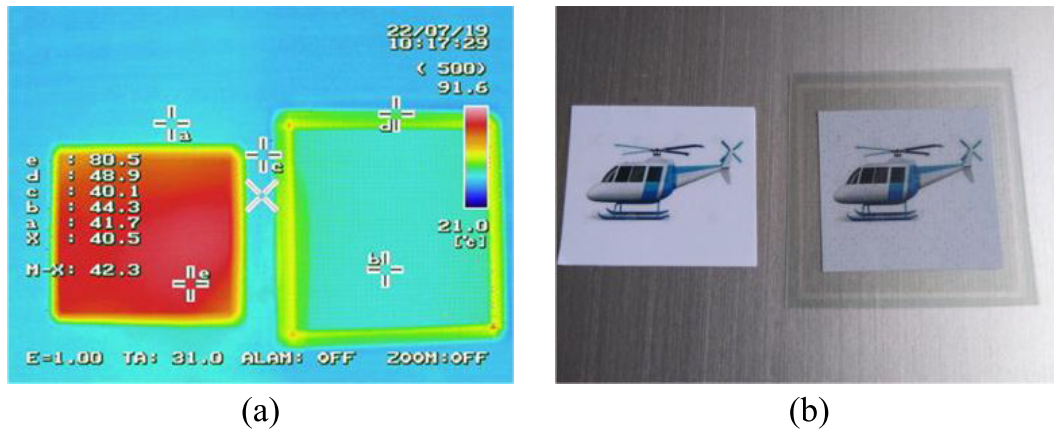


Figure 10. (a) IR photograph (b) visible photograph of the IRSL.

difficult to obtain the simulated emissivity of radar-IR bi-stealth structure. Therefore, only the experimental discussion results are given here. According to the Kirchhoff's law, the emission of the material is equal to the absorption under equilibrium conditions. Therefore, we can obtain the IR emissivity through measuring the reflection spectra of the structure. The Vertex 80 was used in the measurement of IR band reflection. The emissivity of the sample is shown in figure 9 which was calculated from the measured reflection. It can be seen that the average emissivity is about 0.30 in the IR band of 3 μm –14 μm .

To check the IR stealth property of the structure, a 40 mm \times 40 mm IRSL sample was fabricated for IR radiation measurement. Also, one piece of paper without any covering was used as the reference sample. They were placed on a thermal plate and heated simultaneously. These samples consequently had the same temperature. Their thermal IR images were measured by a thermal camera operating in the range of 8–14 μm . As shown in figure 9, the high temperature paper shows very strong IR emission, and it is easily detected by IR detection equipment. The experimental temperature of our IRSL sample and paper are 44.3 $^{\circ}\text{C}$ and 80.5 $^{\circ}\text{C}$, respectively. The temperature of metallic thermal plate is 41.7 $^{\circ}\text{C}$. It can be observed that the emissivity of the proposed IRSL structure is close to that of the metal. The corresponding visible light photograph is given in figure 10(b). The surface emissivity of IRSL can be calculated by the equation [37]

$$\varepsilon = (T_r^4 - T_a^4)/(T_o^4 - T_a^4) \quad (6)$$

where T_r is the temperature measured by the IR thermal camera (44.3 $^{\circ}\text{C}$), T_a is the ambient temperature (27 $^{\circ}\text{C}$), and T_o is the true temperature (80.5 $^{\circ}\text{C}$). According to the equation (1), the IR emissivity of the proposed IRSL structure is calculated approaching 0.27. The calculated result value of 0.27 is close to the measured value of 0.30.

4. Conclusions

In conclusion, an optical transparent metamaterial structure has been designed and fabricated to achieve radar-IR stealth-compatibility. Two special metasurfaces that can achieve

high-efficiency microwave absorption and low IR emission are designed and combined to realize the desired functionality. All the layers are designed based on transparent conductive ITO-coated-PET film substrate with different sheet resistances. The IRSL was composed of ITO square patch array and nearly transparent to microwaves with a frequency lower than 18 GHz. The corresponding microwave transmissivity is greater than 91%. The emissivity of the IRSL is as low as 0.30 in 3 μm –14 μm IR band, which satisfies the requirements of IR stealth. In addition, our proposed radar-IR bi-stealth structure has high absorptivity larger than 90% from 6 to 18 GHz within a wide incident angle of $\pm 40^{\circ}$. Contributed to the optically transparent ITO-coated-PET films and PMMA dielectric, the measured optical transmittance is approximately 75.02%. In general, this research provides a new method to achieve multifunctional stealth technology.

Acknowledgments

This work is supported by the National Natural Science Foundation of China (Grant Nos. 61331005, 61801509, 61771485, 61671467). Research Found of Department of Basic Sciences at Air Force Engineering University (JK2019207).

ORCID iDs

Cuilian Xu <https://orcid.org/0000-0003-0396-5548>
 Yongqiang Pang <https://orcid.org/0000-0001-8403-6294>
 Wenjie Wang <https://orcid.org/0000-0001-9649-3011>
 Yueyu Meng <https://orcid.org/0000-0003-4077-3975>

References

- [1] Rao G A and Mahulikar S P 2002 Integrated review of stealth technology and its role in airpower *Aeronaut. J.* **106** 629–42
- [2] Qi D, Wang X, Cheng Y Zh, Gong R Zh and Li B W 2016 Design and characterization of one-dimensional photonic crystals based on ZnS/Ge for infrared-visible compatible stealth applications *Opt. Mater.* **62** 52–6

- [3] Immordino M L, Dosio F and Cattel L 2006 Stealth liposomes: review of the basic science, rationale, and clinical application existing and potential *Int. J. Nanomed.* **1** 3
- [4] Pang Y Q, Shen Y, Li Y F, Wang J F, Xu Zh and Qu Sh B 2018 Water-based metamaterial absorbers for optical transparency and broadband microwave absorption *J. Appl. Phys.* **123** 155106
- [5] Kim J, Han K and Hahn J W 2017 Selective dual-band metamaterial perfect absorber for infrared stealth technology *Sci. Rep.* **7** 6740
- [6] Kluskens M S and Newman E H 1990 Scattering by a chiral cylinder of arbitrary cross section *IEEE Trans. Antennas Propag.* **38** 1448
- [7] Fu Q, Wang W, Li D and Pan J 2014 Research on surface modification and infrared emissivity of In_2O_3 :W thin films *Thin Solid Films* **570** 68
- [8] Phan L, Walkup W G IV, Ordinario D D, Karshalev E, Jocson J M, Burke A M and Gorodetsky A A 2013 Reconfigurable infrared camouflage coatings from a cephalopod protein *Adv. Mater.* **25** 5621–5
- [9] Xiao L, Ma H, Liu J, Zhao W, Jia Y, Zhao Q and Jiang K 2015 Fast adaptive thermal camouflage based on flexible VO_2 /graphene/CNT thin films *Nano Lett.* **15** 8365–70
- [10] Liu J W, Wang J J and Gao H T 2018 Infrared emissivities and microwave absorption properties of perovskite $\text{La}_{1-x}\text{Ca}_x\text{MnO}_3$ ($0 \leq x \leq 0.5$) *Mater. Sci. Forum* **914** 96–101
- [11] Wang Zh X, Cheng Y Zh, Nie Y, Wang X and Gong R Zh 2014 Design and realization of one-dimensional double hetero-structure photonic crystals for infrared-radar stealth-compatible materials applications *J. Appl. Phys.* **116** 054905
- [12] Shen X, Cui T J and Zhao J 2011 Polarization-independent wide-angle triple-band metamaterial absorber *Opt. Express* **19** 9401–7
- [13] Zhao J, Cheng Q, Chen J, Qi M Q, Jiang W X and Cui T J 2013 A tunable metamaterial absorber using varactor diodes *New J. Phys.* **15** 043049
- [14] Ding F, Cui Y, Ge X, Zhang F, Jin Y and He S 2012 Ultra-broadband microwave metamaterial absorber *Appl. Phys. Lett.* **100** 103506
- [15] Zhang C, Cheng Q, Yang J, Zhao J and Cui T J 2017 Broadband metamaterial for optical transparency and microwave absorption *Appl. Phys. Lett.* **110** 143511
- [16] Pu M, Hu C, Wang M, Huang C, Zhao Z, Wang C, Feng Q and Luo X 2011 Design principles for infrared wide-angle perfect absorber based on plasmonic structure *Opt. Express* **19** 17413–20
- [17] Huang L, Chowdhury D R, Ramani S, Reiten M T, Luo S N, Taylor A J and Chen H T 2012 Experimental demonstration of terahertz metamaterial absorbers with a broad and flat high absorption band *Opt. Lett.* **37** 154–6
- [18] Cui Y, Fung K H, Xu J, Ma H, Jin Y, He S and Fang N X 2012 Ultrabroadband light absorption by a sawtooth anisotropic metamaterial slab *Nano Lett.* **12** 1443–7
- [19] Wang W J, Wang J, Yan M B, Wang J F, Ma H, Feng M D and Qu Sh B 2018 Dual band tunable metamaterial absorber based on cuboid ferrite particles *J. Phys. D: Appl. Phys.* **51** 315001
- [20] Tian H, Liu H T and Cheng H F 2014 A thin radar-infrared stealth-compatible structure: design, fabrication, and characterization *Chin. Phys. B* **23** 025201
- [21] Zhang C, Yang J, Yuan W, Zhao J, Dai J Y, Guo T C, Liang J, Xu G Y, Cheng Q and Cui T J 2017 An ultralight and thin metasurface for radar-infrared bi-stealth applications *J. Phys. D: Appl. Phys.* **50** 444002
- [22] Pang Y Q, Li Y F, Yan M B, Liu D Q, Wang J F, Xu Zh and Qu Sh B 2018 Hybrid metasurfaces for microwave reflection and infrared emission reduction *Opt. Express* **26** 11950–8
- [23] Shrestha S, Wang Y, Overvig A, Lu M, Stein A, Negro L D and Yu N F 2018 Indium tin oxide broadband metasurface absorber *ACS Photonics* **10** 3526–33
- [24] Song G Y, Zhang C, Cheng Q, Jing Y, Qiu C G and Cui T J 2018 Transparent coupled membrane metamaterials with simultaneous microwave absorption and sound reduction *Opt. Express* **26** 22916–25
- [25] Lai S F, Wu Y H, Wang J J, Wu W and Gu W H 2018 Optical-transparent flexible broadband absorbers based on the ITO-PET-ITO structure *Opt. Mater. Express* **8** 1585–92
- [26] Deng R X, Li M L, Muneer B, Zhu Q, Shi Z Y, Song L X and Zhang T 2018 Theoretical analysis and design of ultrathin broadband optically transparent microwave metamaterial absorbers *Materials* **11** 107
- [27] Jing H B, Ma Q, Bai G D, Bao L, Luo J and Jun C T 2018 Optically transparent coding metasurfaces based on indium tin oxide films *J. Appl. Phys.* **124** 023102
- [28] Chen K, Cui L, Feng Y J, Zhao J M, Jiang T and Zhu B 2017 Coding metasurface for broadband microwave scattering reduction with optical transparency *Opt. Express* **25** 5571–9
- [29] Xu C L, Wang B K, Pang Y Q, Wang J F, Yan M B, Wang W J, Wang A X, Jiang J M and Qu Sh B 2019 Hybrid metasurfaces for infrared-multiband radar stealth-compatible materials applications *ACCESS* **7** 147586
- [30] Zhang Ch L et al 2019 Flexible and transparent microwave–infrared bistealth structure *Adv. Mater. Technol.* **4** 1900063
- [31] Zhao J, Zhang Ch, Cheng Q, Yang J and Cui T J 2018 An optically transparent metasurface for broadband microwave antireflection *Appl. Phys. Lett.* **112** 073504
- [32] Pang Y Q, Zhou Y J and Wang J 2011 Equivalent circuit method analysis of the influence of frequency selective surface resistance on the frequency response of metamaterial absorbers *J. Appl. Phys.* **110** 023704
- [33] Bhattacharyya S, Ghosh S and Srivastava K V 2014 Equivalent circuit model of an ultra-thin polarization independent triple band metamaterial absorber *AIP Adv.* **4** 097127
- [34] Shang Y P, Shen Zh X and Xiao Sh Q 2013 On the design of single-layer circuit analog absorber using double-square-loop array *IEEE Trans. Antennas Propag.* **61** 6022–9
- [35] Zadeh A K and Karlsson A 2009 Capacitive circuit method for fast and efficient design of wideband radar absorbers *IEEE Trans. Antennas Propag.* **57** 2307–14
- [36] Ghosh S and Srivastava K V 2014 An equivalent circuit model of FSS based metamaterial absorber using coupled line theory *IEEE Antennas Wireless Propag. Lett.* **14** 511–4
- [37] Ghosh S, Bhattacharyya S, Kaiprath Y and Srivastava K V 2014 Bandwidth-enhanced polarization-insensitive microwave metamaterial absorber and its equivalent circuit model *J. Appl. Phys.* **115** 104503
- [38] Zhong Sh M, Jiang W, Xu P P, Liu T J, Huang J F and Ma Y G 2017 A radar-infrared bi-stealth structure based on metasurfaces *Appl. Phys. Lett.* **110** 063502